PRESSURE BROADENING AND SHIFT OF THE 326.1 nm Cd LINE PERTURBED BY H_2 AND D_2

A. Bielski, R. Ciuryło, J. Domysławska, D. Lisak, R.S. Trawiński and J. Wolnikowski

Institute of Physics, Nicholas Copernicus University
Grudziądzka 5/7, 87-100 Toruń, Poland

(Received December 13, 1999: in final form February 3, 2000)

The experimental values of pressure broadening and shift coefficients of the ^{114}Cd 326.1 nm line perturbed by H_2 and D_2 are determined using a LIF technique and compared with theoretical values calculated from the impact theory.

PACS numbers: 32.70.–n, 33.70.–w, 34.20.–b

1. Introduction

In a series of experiments in our laboratory [1–5] the pressure broadening and shift of the ^{114}Cd 326.1 nm ($5\,^1S_0$-$5\,^3P_1$) intercombination line perturbed by He, Ne, Ar, Kr, and Xe have been studied using a pressure-scanned Fabry–Perot interferometer. As a sequel to the previous papers this paper reports results of measurements of the pressure broadening and shift of this line caused by the simplest molecular perturbers such as H_2 and D_2. There are only a few papers in the literature dealing with collisional effects on the 326.1 nm Cd line perturbed by molecular gases but they have rather a qualitative character [6–8]. The study of the pressure broadening and shift of the 326.1 nm Cd line by various molecular gases is of interest as it can provide information on the interaction between the ground-state perturbing molecules and the excited ($5\,^3P_1$) Cd-atom. The main goal of this work is to establish magnitudes of the broadening and shift coefficients of the 326.1 nm Cd line perturbed by H_2 and D_2 at low perturbing gas pressures, i.e. in the linear region where two-body interactions predominate and the impact approximation of the collisional broadening theory is fully applicable.

Due to the known high quenching rate for the Cd–H_2 and Cd–D_2 systems [9–11], present measurements were performed with a laser induced fluorescence (LIF) technique.

2. Experimental setup

Our measurements were performed using a ^{114}Cd isotope. The cells containing the cadmium were filled with perturbing gas and cut-off from the vacuum system. The perturbing gas pressure was between 1.5 and 30 Torr at room temper-

ature. Each cell was situated in an oven at a temperature of 450 K. Line shapes of the cadmium 326.1 nm line were registered using a digital laser spectrometer. The intensity of fluorescence emitted perpendicularly to the incident laser beam was detected as the laser frequency was scanned across the line. The total fluorescence signal was measured by a thermoelectrically cooled photomultiplier (EMI 6256 B) working in the photon counting mode characterized by a very good signal-to-noise ratio.

The experimental set-up is shown in Fig. 1. An actively stabilized single--frequency COHERENT CR 899-21 ring dye laser, operating on DCM dye was pumped by INNOVA-308 argon-ion laser. The ring laser was equipped with an intracavity frequency doubler CR 8500 (with $LiIO_3$ crystal) and provided single mode UV output continuously tunable for up to 60 GHz. The line width of this laser line was about 1 MHz. Ring laser frequency is scanned by changing the peak transmission of its reference cavity. This is done by changing the optical path length of the reference cavity with a galvo-controlled scanning Brewster plate. The laser frequency as a function of angle of rotation of the scanning Brewster plate is highly reproducible but not quite linear [12]. To compensate this effect it is necessary to perform frequency calibration. CR 899-21 ring laser operating with frequency doubler can simultaneously emit the UV line as well as deliver its fundamental (red) line. This red line was directed to a confocal Fabry–Perot interferometer (FPI) with a free spectral range of 1.5 GHz and to the 100 cm long iodine cell operated at a temperature of 35°C. Phase sensitive detection was employed to monitor the FPI peaks intensity. An EG&G model 7260 DSP digital lock-in amplifier was used in conjunction with a frequency programmable EG&G 197 light chopper and silicon photodiode. The iodine absorption signal was monitored using silicon photodiode and digital multimeter (DMM). The FPI transmission peaks

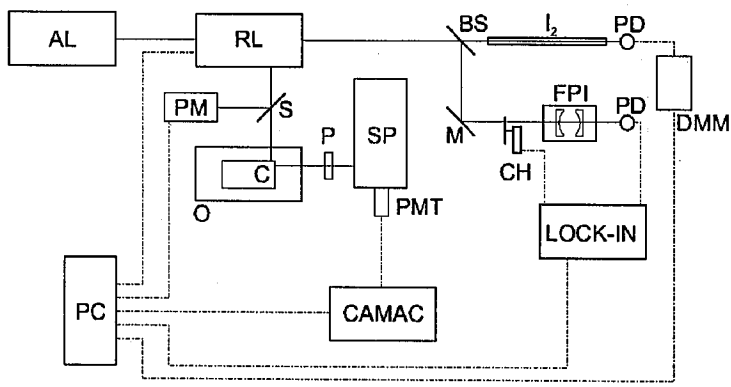

Fig. 1. The experimental set up: AL — argon laser, RL — ring dye laser with frequency doubler, PM — laser power meter, O — oven, C — cell, P — polarizer, SP — monochromator, PMT — photomultiplier, S — semaphore shutter with mirror, CAMAC — electronic system, BS — beam splitter, I_2 — iodine cell, M — mirror, CH — light chopper, FPI — confocal Fabry–Perot interferometer, PD — photodiode, DMM — digital multimeter, LOCK-IN — lock in amplifier, PC — computer, solid line — light beams, dash-and-dot line — electrical connections.

and I_2 absorption spectrum were recorded simultaneously with the fluorescence signal for frequency calibration. Laser UV output power was monitored using the COHERENT LABMASTER+ power meter equipped with LM-2 UV head. Because the incident laser UV beam was linearly polarized in the vertical direction the collection optics arm contained a linear polarizer set at the "magic angle" (rotated 54.7° from the vertical), so the collection optics system was insensitive to effects due to anisotropy of fluorescence [13–17]. The photon counting process was performed by an electronic system built in the CAMAC standard described elsewhere [1].

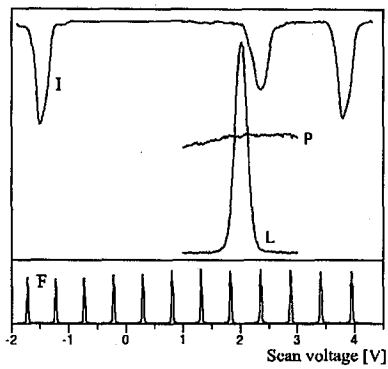

Fig. 2. Typical raw data set of the Cd 326.1 nm line perturbed by D_2 at a pressure of 10 Torr taken during a single laser scan: L — LIF signal, P — laser UV output power, I — iodine absorption spectra, F — FPI peaks.

We acquired the data with a PC computer. The computer generated the step-like voltage that scanned the laser up to 60 GHz. For every step the computer collected signals from the photomultiplier, photodiodes, and power meter. Figure 2 shows a typical data set from a single laser scan. The horizontal axis shows the values of the scanning voltage. The computer then converted the Fabry–Perot markers into a wave number scale, whose value was determined from the position of the iodine peaks [18, 19]. As can be seen from Fig. 2 the laser UV output power varies with the laser scan. Therefore, before the numerical evaluation, the registered line profile is renormalised according to the measured laser UV power.

3. Data analysis

In the case of the Cd–H_2 and Cd–D_2 systems the observed line profile at low pressures may be given by Voigt profile $I_V(\tilde{\nu})$ which is a convolution of the Lorentzian and Gaussian components. In our analysis we also have to take into account the background signal I_B. The resultant line shape profile can be written in the following form:

$$I_V(\tilde{\nu}) = I_B + A \int_{-\infty}^{+\infty} \frac{\exp\left[-4\,(y/\gamma_D)^2 \ln 2\right]}{(\tilde{\nu} - \tilde{\nu}_0 - \Delta - y)^2 + (\gamma_L/2)^2} dy, \tag{1}$$

where

$$A = I_M \left\{ \int_{-\infty}^{+\infty} \frac{\exp\left[-4\,(y/\gamma_D)^2 \ln 2\right]}{y^2 + (\gamma_L/2)^2} \mathrm{d}y \right\}^{-1} \tag{2}$$

and I_M is the intensity in the line peak, $\tilde{\nu}_0$ is the unperturbed wave number of the line, Δ is the line shift, γ_L and γ_D are halfwidths (FWHM) of the Lorentzian and Gaussian components of the observed profile, respectively.

The profile (1) was fitted to our measured profiles using the Marquardt algorithm [20] for a least-squares estimation of nonlinear parameters. The fitting parameters were the Lorentzian (γ_L) and Gaussian (γ_D) halfwidths, the line shift (Δ), the A-factor, and the background signal I_B.

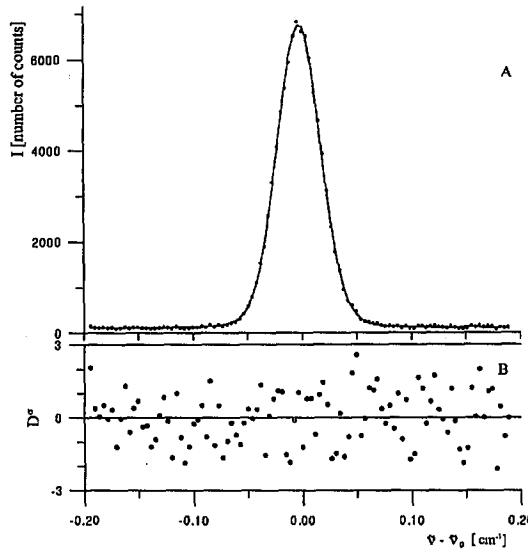

Fig. 3. The shape of the Cd 326.1 nm line perturbed by D_2 at a pressure of 10 Torr: (A) experimental points together with the best-fit theoretical profile (full curve), (B) the weighted differences D^σ between experimental and fitted profiles.

An example of an experimental profile of the Cd 326.1 nm line perturbed by D_2 at a pressure of 10 Torr is shown in Fig. 3A. Figure 3B shows residues in the form of the weighted differences $D^\sigma = (I_{exp} - I_V)/\sqrt{I_V}$ between the experimental (I_{exp}) and fitted (I_V) profile. As can be seen the residues indicate the random noise only with no evidence of systematic departures between the theoretical and experimental profiles.

4. Results and discussion

The experimental values of the Doppler halfwidths of the 326.1 nm ^{114}Cd line perturbed by H_2 and D_2 determined on the basis of the Voigt analysis are shown in Fig. 4, where they are plotted as a function of pressure. The average Doppler halfwidths γ_D for Cd–H_2 and Cd–D_2 systems were found to be

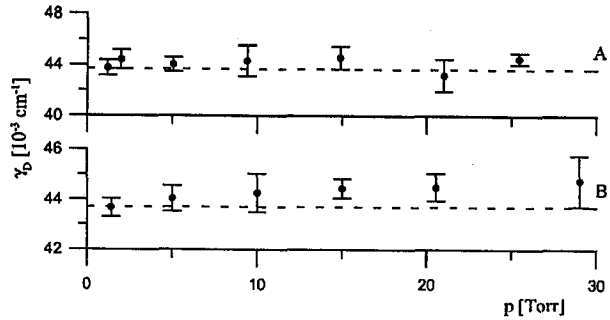

Fig. 4. Plots of the Doppler γ_D halfwidths for: (A) Cd–H_2 and (B) Cd–D_2 systems against perturbing gas pressure. Dashed line — theoretical Doppler halfwidth corresponding to the cell temperature (450 K). Error bars indicate the value of the standard deviation.

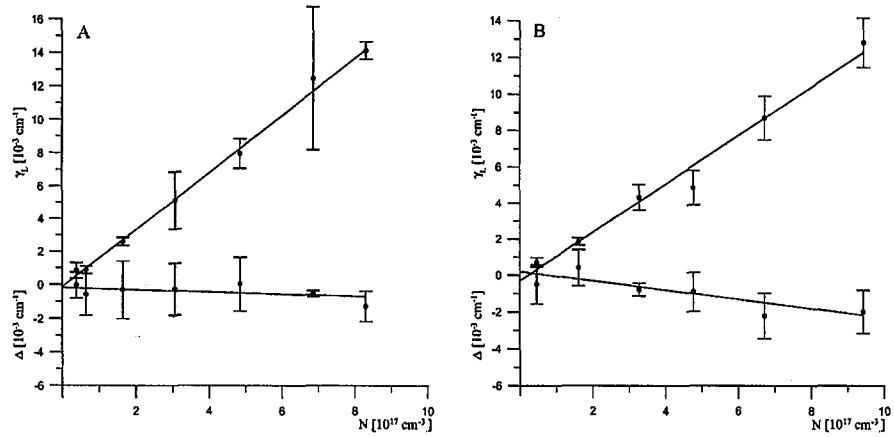

Fig. 5. Plots of the Lorentzian γ_L halfwidth and shift Δ for the 326.1 nm Cd line against the density N of H_2 (A) and D_2 (B). Error bars indicate the value of the standard deviation.

$(44.2 \pm 0.9) \times 10^{-3}$ cm^{-1} and $(44.2 \pm 0.7) \times 10^{-3}$ cm^{-1}, respectively. These average values agree with theoretical Doppler halfwidth 43.7×10^{-3} cm^{-1} corresponding to the cell temperature (450 K).

The Lorentzian halfwidths γ_L and shifts Δ determined from the Voigt analysis are shown in Fig. 5, where they are plotted as functions of the perturbing gas density N. As can be seen both the Lorentzian halfwidth γ_L and shift Δ are linearly dependent on N. These dependences can be described by the relations

$$\gamma_L = \gamma_L^{(0)} + \beta N, \tag{3}$$

$$\Delta = \Delta^{(0)} + \delta N, \tag{4}$$

where β and δ are the pressure broadening and shift coefficients, respectively. Here $\gamma_L^{(0)}$ and $\Delta^{(0)}$ are the residual halfwidth and shift of the line. It should be noted that in our fitting procedure we used an arbitrary value of unperturbed wave number $\tilde{\nu}_0$ chosen to get the residual value $\Delta^{(0)}$ close to zero for both systems

under investigation. In our experiment we found for the Cd–H_2 system $\gamma_L^{(0)} = (-0.13 \pm 0.31) \times 10^{-3}$ cm^{-1} and the residual value $\Delta^{(0)}$ of the line shift was found to be equal to $(-0.19 \pm 0.34) \times 10^{-3}$ cm^{-1}. For the Cd–D_2 system we found $\gamma_L^{(0)} = (-0.31 \pm 0.26) \times 10^{-3}$ cm^{-1} and $\Delta^{(0)} = (0.19 \pm 0.35) \times 10^{-3}$ cm^{-1}. This means that the residual values are close to zero in the framework of standard deviation. The experimental values of the pressure broadening β and shift δ coefficients are listed in Table I.

TABLE I

The experimental and calculated values of the β and δ coefficients (in units 10^{-20} cm^{-1}/atom cm^{-3}). For experimental data the values of the standard deviations are given.

Cd–H_2	β	δ
Experimental	1.73 ± 0.08	-0.06 ± 0.09
van der Waals	1.42	−0.52
Cd–D_2		
Experimental	1.34 ± 0.06	-0.25 ± 0.07
van der Waals	1.15	−0.42

In order to interpret our experimental data we calculated broadening β and shift δ coefficients from the impact theory assuming the interaction potential in the van der Waals form

$$V(R) = -\frac{C_6}{R^6}, \tag{5}$$

where C_6 is a constant depending on the quantum numbers of energy levels of Cd-atom and polarizability α of the perturbing molecule.

The force constant C_6 can be, in principle, calculated using quantum-mechanical treatment. However, quantum-mechanical calculation of C_6 requires the knowledge of line strengths for all transitions in the radiating atoms which involve the upper and lower states [21]. Because the line strengths for many transitions involving the $5\,^1S_0$ and $5\,^3P_1$ states are not known, the quantum-mechanical calculation of C_6 for the 326.1 nm line is, as yet, impossible. Therefore, in order to estimate C_6 we used here the approximate formula given by Unsöld [22]: $C_6 = \alpha e^2 \langle r^2 \rangle$, where e is the elementary charge and $\langle r^2 \rangle$ is the quantum-mechanical expectation value of r^2 in a given state of radiating atom. The values of $\langle r^2 \rangle$ were calculated using the Coulomb approximation

$$\langle r^2 \rangle = \frac{a_0^2 n_{\text{eff}}^2}{2}[5n_{\text{eff}}^2 + 1 - 3l(l+1)], \tag{6}$$

where n_{eff} denotes the effective quantum number for a given (upper or lower) state. In our calculations for H_2 and D_2 we used the theoretical values of polarizabilities $\alpha_{H_2} = 0.8045 \times 10^{-24}$ cm^3 and $\alpha_{D_2} = 0.794 \times 10^{-24}$ cm^3 calculated by Kołos and Wolniewicz [23]. The values of the C_6 constants obtained in this way are listed in Table II.

TABLE II

Calculated values of C_6 van der Waals constants (in atomic units).

State	$5\,^1S_0$	$5\,^3P_1$
Cd–H_2	35.1	57.6
Cd–D_2	34.7	56.9

The theoretical values of the pressure broadening (β) and shift (δ) coefficients averaged over a Maxwellian distribution of velocities were calculated using the classical phase-shift theory due to Lindholm [24] and Foley [25], which for the van der Waals potential yields

$$\beta = \frac{7.97}{2\pi c}\left(\frac{|\Delta C_6|}{\hbar}\right)^{0.4} \bar{v}^{0.6} \tag{7}$$

and

$$\frac{\delta}{\beta} = 0.363\ \mathrm{sign}(\Delta C_6). \tag{8}$$

Here $\Delta C_6 = C_6^{\mathrm{u}} - C_6^{\mathrm{l}}$ is the difference of force constants for the upper and lower states of Cd-atom involved in the electronic transition giving rise to the 326.1 nm line, $\bar{v}$ is the mean value of relative velocity of the pair Cd atom – perturbing molecule.

The theoretical values of β and δ coefficients obtained from Eqs. (7) and (8) with C_6 calculated using Eq. (6) are listed in Table I where they are compared with experimental data. As it can be seen the theoretical values are in poor agreement with experiment both for Cd–H_2 and Cd–D_2. The agreement is particularly poor in the case of the shift both for Cd–H_2 and Cd–D_2. The cause of these discrepancies may come from two reasons. Firstly, the van der Waals potential does not represent a sufficient approximation for the real potential in the Cd–H_2 and Cd–D_2 systems. Secondly, the conditions of applicability of the classical adiabatic impact theory due to Lindholm and Foley may not be fulfilled for light perturbers such as H_2 and D_2. There is no doubt that the Baranger [26] quantum-mechanical theory is fully applicable for them, but its application requires the knowledge of the accurate interaction potentials. Moreover, it should be emphasized that in the description of interactions in the Cd-molecular gas systems one should take into account not only the distance R between the Cd atom and perturbing molecule but also the spatial orientation of the perturbing molecule. The R-dependent potential curve should then be replaced by a potential surface. Unfortunately, such potential surfaces for the Cd–H_2 and Cd–D_2 systems for Cd in its ground ($5\,^1S_0$) and excited ($5\,^3P_1$) states are not known as yet.

Acknowledgment

The authors wish to express their gratitude to Prof. J. Szudy for fruitful discussions and valuable help in the preparation of the manuscript.

This work was supported by the grant No. 673/PO3/96/10 (2 PO3B 005 10) from the Committee for Scientific Research.

References

[1] A. Bielski, S. Brym, R. Ciuryło, J. Domysławska, E. Lisicki, R.S. Trawiński, *J. Phys. B, At. Mol. Opt. Phys.* **27**, 5863 (1994).

[2] A. Bielski, S. Brym, R. Ciuryło, J. Domysławska, R.S. Trawiński, M.G. Lednev, *Acta Phys. Pol. A* **90**, 1155 (1996).

[3] S. Brym, R. Ciuryło, E. Lisicki, R.S. Trawiński, *Phys. Scr.* **56**, 541 (1996).

[4] S. Brym, J. Domysławska, *Phys. Scr.* **52**, 511 (1995).

[5] S. Brym, R. Ciuryło, R.S. Trawiński, A. Bielski, *Phys. Rev. A* **56**, 4501 (1997).

[6] A.S. Bazov, A.W. Zerebenko, *Zh. Prikl. Spektrosk.* **12**, 403 (1970).

[7] R. Pepperl, *Z. Naturforsch. A* **25**, 927 (1970).

[8] I.L. Greenstein, D.A. Kackov, M.A. Hodorovsky, *Zh. Prikl. Spektrosk.* **44**, 728 (1986), [*J. Appl. Spectrosc.* **44**, 439 (1986)].

[9] M. Czajkowski, E. Walentynowicz, L. Krause *J. Quant. Spectrosc. Radiat. Transf.* **28**, 13 (1982).

[10] M. Czajkowski, A. Bączyński, L. Krause, *J. Quant. Spectrosc. Radiat. Transf.* **31**, 491 (1984).

[11] H.P. Dirda, M. Baumann, *Z. Phys. D* **25**, 107 (1993).

[12] *Ring Dye Laser Systems, The Essence of Innovation*, Coherent, Laser Products Division, Palo Alto (USA) 1988.

[13] R.E. Walkup, A. Spielfiedel, D.E. Pritchard, *Phys. Rev. Lett.* **45**, 986 (1980).

[14] R.E. Walkup, B. Stewart, D.E. Pritchard, *Phys. Rev. A* **29**, 169 (1984).

[15] M. Harris, E.L. Lewis, D. McHugh, I. Shannon, *J. Phys. B* **19**, 3207 (1986).

[16] R.J. Ballagh, J. Cooper, *Astrophys. J.* **213**, 479 (1977).

[17] V. Kroop, W. Behmenburg, *Z. Phys. A* **294**, 299 (1980).

[18] S. Gerstenkorn, P. Luc, *Atlas du Spectre d'Absorption de la Molecule d'Iode*, Editions du C.N.R.S., Paris 1978.

[19] S. Gerstenkorn, P. Luc, *Rev. Phys. Appl.* **14**, 791 (1979).

[20] D.W. Marquardt, *J. Soc. Industr. Appl. Math.* **11**, 431 (1963).

[21] J. Fiutak, M. Frąckowiak, *Bull. Acad. Polon. Sci. Ser. Sci. Math. Astr. Phys.* **11**, 175 (1963).

[22] A. Unsöld, *Physik der Sternatmospharen*, Springer, Berlin 1955.

[23] W. Kołos, L. Wolniewicz, *J. Chem. Phys.* **46**, 1426 (1967).

[24] E. Lindholm, *Ark. Mat. Astr. Fys. B* **28**, No. 13 (1941).

[25] H.M. Foley, *Phys. Rev.* **69**, 616 (1946).

[26] M. Baranger, *Phys. Rev.* **111**, 494 (1958); **112**, 855 (1958).